AUTEX Research Journal, Vol. 22, No 1, March 2022, DOI 10.2478/aut-2021-0003

NUMERICAL SIMULATION OF FIBER MOTION IN THE CONDENSING ZONE OF LATERAL COMPACT SPINNING WITH PNEUMATIC GROOVE

Jindan Lyu[1], Longdi Cheng[1], *, Bugao Xu[2,] *, Zhihong Hua[3]

1 Key Laboratory of Textile Science & Technology, Ministry of Education, College of Textiles, Donghua University, Shanghai 201620, China
2 Department of Merchandising and Digital Retailing University of North Texas, Denten, Texas, TX76201, the United States of America
3 College of Science, Donghua University, Shanghai 201620, China
*Corresponding author: Longdi Cheng, email: ldch@dhu.edu.cn; Bugao Xu, email: bugao.xu@unt.edu

Abstract:

Lateral compact spinning with pneumatic groove is a spinning process to gather fibers by common actions of airflow and mechanical forces. Compared with ring spinning, it can more effectively reduce yarn hairiness and enhance yarn strength. However, fiber motion in the agglomeration area is complex. And, it is important to establish a new fiber model to accurately describing the fiber motion. The objectives of this research were to create a new fiber model to simulate the agglomeration process, to analyze yarn properties of the lateral compact spinning with pneumatic groove, and to compare with other spinning yarns through a series of tests. The new fiber model was based on the finite element method implemented in MATLAB and was to show the fiber motion during the agglomeration area. The simulation generated results were close to the real motion of fibers in spinning. In the lateral compact spinning with pneumatic groove, fiber bundle through the agglomeration area can be gathered, and the output of the fiber bundle was nearly to cylinder before yarn twisted. The experiments demonstrated that the lateral compact spinning with pneumatic groove can improve the yarn properties: increase the yarn twist, enhance the yarn strength, and reduce the yarn hairiness.

Keywords:

Compact spinning; fiber motion; agglomeration process; yarn properties

1. Introduction

Spinning plays an important role in determining the mechanical properties of yarns. And, fiber motion is important for the theoretical research for yarn generation during the spinning process. Yarn is a linear assembly of twisted short fibers or filaments [1]. In order to describe the fiber motion during spinning, a fiber model needs to be established. Fiber is a flexible continuum material with certain elasticity and a large length–diameter ratio. When a fiber is considered as an elastic thin rod, the multiple segments can be deformed relative to others. Thus, the motion of a fiber in the airflow field is nonlinear with large deformation [2]. In the past decades, a fiber was usually simplified by a variety of mechanical models for fiber property characterization, particularly with particles or rigid cylindrical rods being model's elements. For instance, a chain model was used to simplify a fiber into many hinged short rigid rods [3-4]. However, a simple model may not be effective enough to describe the physical characteristics of fibers [5]. In the late 1980s, mechanical modeling of fiber had made some breakthroughs because of widespread applications of computer. Cheng established a series of mechanical models with multiple spheres for fibers, containing almost all the physical characteristics of fibers [6-7]. But, the expression of the mechanical behaviors from these models was not applicable for fibers in the airflow field. In the 1990s, many scholars continued to study the mechanical models of fiber. Yamamoto and Matsuoka proposed a bead-spring-chain model, which was similar to a polymer chain; it can better describe the rigidity and flexibility of fiber [8]. Zeng and Wang improved this model, but it could not be applied to fibers of a large length–diameter ratio (about 1000:1), and its computation was rather complex and difficult [9,10,11].

In this article, we present a finite element model with continuous elastic fine rods established in MATLAB to simulate the motion of fiber in the three-dimensional space. In this model, a fiber is regarded as the elastic thin rod, and it is used to simulate the large deformation and to analyze the influence of its axial force on the bending. From this new finite element model, the fiber movement can be calculated and visualized, and the simulation result can be more closely to the real fiber movement.

2. Numerical simulation of fiber motion

In order to describe the fiber movement during the gathering zone in the spinning process, a proper mathematical model for fibers should be established to numerically simulate the statics of the fiber under lateral mechanical force in the general stress state. This fiber model regards a fiber as elastic fine rods so that the finite element method can be used to solve the nonlinear large deformation of an elastic thin rod.

2.1. Fiber finite model and simulation

In this paper, we compared the fiber movement of lateral entry compact spinning with pneumatic groove, intermediate entry compact spinning with suction groove, and ring spinning. First, we used the Ansys 15.0 to get the velocity of fiber bundle and then established the fiber finite element model by MATLAB. Finally, we simulated the fiber motion in the agglomeration area.

In the new fiber finite element model, the fiber was regarded as an elastic thin rod. The whole elastic thin rod was decomposed into a combination of micro-section rigid mass unit and massless elastic rod unit, and the analysis of the elastic thin rod by finite element method was carried out. The deformation of the rod unit in three-dimensional space can be decomposed into axial tensile deformation and the combination of bending and torsional deformation in two principal planes.

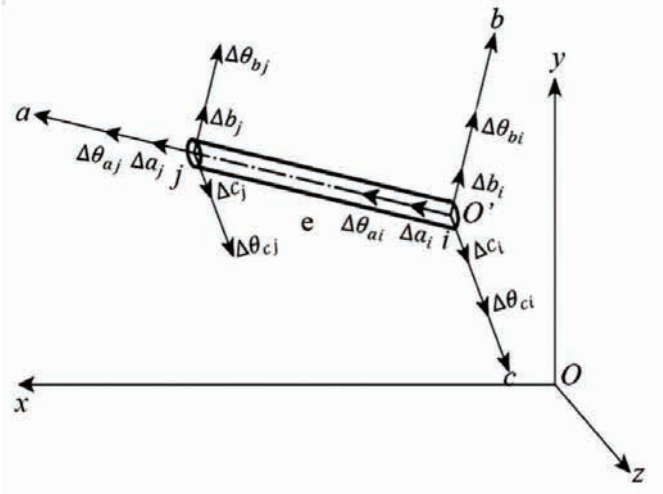

Figure 1. The spatial bar element and coordinate system

Figure 1 showed the establishment of an overall coordinate system O-xyz for the entire elastic thin rod. The local coordinate system of each rod unit was O'-abc, a was the axis direction of the rod unit, aO'b and aO'c were the two principal plane orientations of the rod unit. The node i and node j were the ends of rod unit e, each of the nodes had six degrees of freedom (displacement component). After the elastic rod unit was deformed by force, the relative displacement of node i in the local coordinate system was calculated by the following formula:

$$\{\bar{\Delta}_i\}^e = \{\Delta a_i, \Delta b_i, \Delta c_i, \Delta\theta_{ai}, \Delta\theta_{bi}, \Delta\theta_{ci}\}^T \quad (1)$$

where Δa_i means the axial displacement of node *i*, Δb_i and Δc_i mean the bending deflection in two transversely curved principle planes, $\Delta\theta_{ai}$ means the torsion angle of the cross-section of the node, $\Delta\theta_{bi}$ and $\Delta\theta_{ci}$ mean the two laterally curved bending corners in the main plane.

In the meantime, the relative displacement of node j in the local coordinate system was calculated by the following formula:

$$\{\bar{\Delta}_j\}^e = \{\Delta a_j, \Delta b_j, \Delta c_j, \Delta\theta_{aj}, \Delta\theta_{bj}, \Delta\theta_{cj}\}^T \quad (2)$$

The displacement of the two nodes of the rod unit in the local coordinate system was calculated by the following formula:

$$\{\bar{\Delta}\}^e = \begin{Bmatrix}\bar{\Delta}_i \\ \bar{\Delta}_j\end{Bmatrix} \quad (3)$$

The force received by node i and node j in the unit local coordinate system was calculated by the following formula:

$$\{\bar{F}_i\}^e = \{Fa_i, Fb_i, Fc_i, M_{ai}, M_{bi}, M_{ci}\}^T \quad (4)$$

$$\{\bar{F}_j\}^e = \{Fa_j, Fb_j, Fc_j, M_{aj}, M_{bj}, M_{cj}\}^T \quad (5)$$

where Fa_i , Fb_i , Fc_i and Fa_j , Fb_j , Fc_j were the force of the node; M_{ai} , M_{bi} , M_{ci} and M_{aj} , M_{bj} , M_{cj} were the force couple of the node.

The combination of forces received by the two nodes of the rod unit was called the rod end force. It was calculated by the following formula:

$$\{\bar{F}\}^e = \begin{Bmatrix}\bar{F}_i \\ \bar{F}_j\end{Bmatrix} \quad (6)$$

Figure 2 showed the connection of quality spatial elastic rod unit. The external force on the elastic thin rod was simplified to the node coordinate system on the node. Each node coordinate system had six degrees of freedom with respect to the fixed global coordinate system. There were six independent coordinate parameters to determine their relative position, and three of them described the moving line displacement of the node, the other three described the angular displacement of the node cross-section. The entire elastic thin rod had 6(n+1) degrees of freedom.

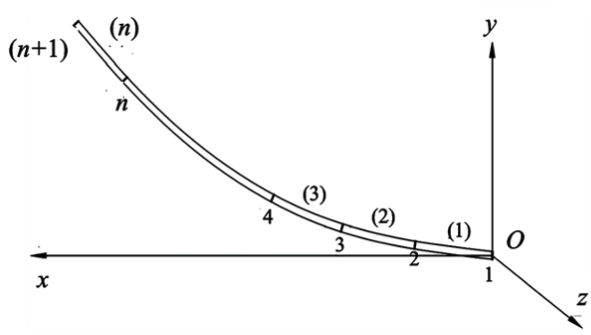

Figure 2. Finite element model of elastic rod element of elastic thin rod

Any general motion of a rigid body in space can be divided into the translation and rotation to its center of mass. According to

the motion theorem of center of mass, the dynamic equation of rigid body moving with the center of mass is:

$$\boldsymbol{ma} = \boldsymbol{F} \tag{7}$$

where: *m* is the mass of the rigid body mass unit; *a* is the absolute acceleration of the mass center relative to the inertial reference frame, where the inertial reference frame is *O-xyz*; and *F* is the principal vector of external force on the rigid body mass element.

The dynamic equation of the motion of mass element of a rigid body in a micro segment around its center of mass in space can be established by using the momentum moment theorem:

$$\boldsymbol{J\alpha} + \boldsymbol{\omega} \times (\boldsymbol{J} \cdot \boldsymbol{\omega}) = \boldsymbol{M} \tag{8}$$

Or

$$\boldsymbol{J\alpha} + \boldsymbol{R} = \boldsymbol{M} \tag{9}$$

where: *J* is the tensor of inertia of the rigid body to the center of mass O.

M is the principal moment of the external force on the rigid body to the center of mass.

$\boldsymbol{\omega}$ is the angular velocity of the rigid body.

$\boldsymbol{\alpha}$ is the derivative of $\boldsymbol{\omega}$ with the coordinate system *O-xyz* to time.

$$\boldsymbol{R} = \boldsymbol{\omega} \times (\boldsymbol{J} \cdot \boldsymbol{\omega})$$

The entire elastic thin rod had 6(n+1) degrees of freedom. So, combining the formulae (7) and (9), it can be written as:

$$\{\boldsymbol{F}_m\} = [\boldsymbol{m}^b]\{\boldsymbol{a}\} + \{\boldsymbol{R}^b\} \tag{10}$$

where $[\boldsymbol{m}^b] = \sum_{i=1}^{n+1} [\boldsymbol{m}^b]^i_{6(n+1)\times 6(n+1)}$

$$\{\boldsymbol{R}^b\} = \sum_{i=1}^{n+1} \{\boldsymbol{R}^b\}^i_{6(n+1)\times 1}$$

The fiber model was established based formula (10) by MATLAB; it was shown as Figures 3 and 4. From that way, the new fiber model was not only can reduce the complex computation but also will more closely to show the characteristic of real fiber.

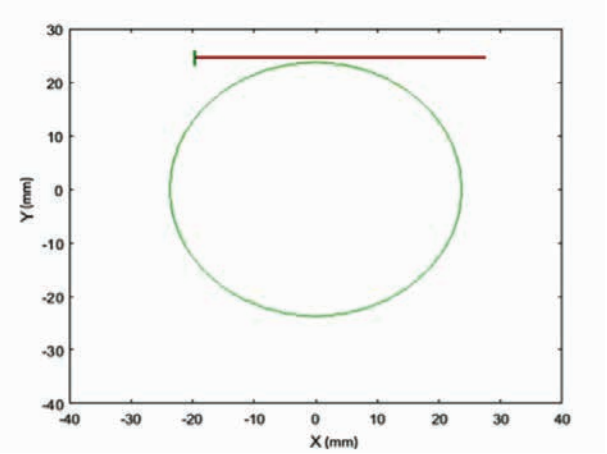

Figure 3. Finite element model of elastic rod element of elastic thin rod

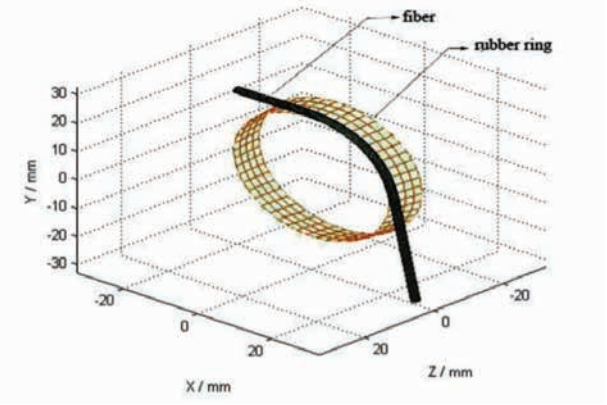

Figure 4. 3D model of fiber agglomeration area

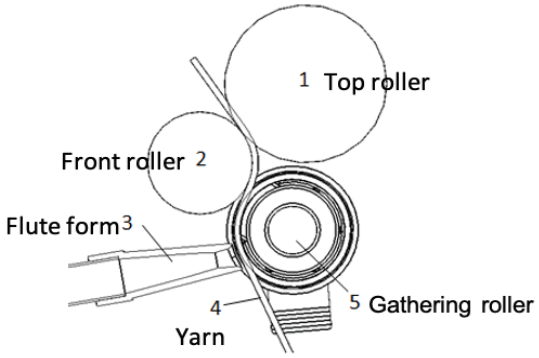

Figure 5. The sketch of lateral entry compact spinning with pneumatic groove

3. Finite element simulation and results

3.1. Initial parameters

The diameter d of the fiber was 0.02 mm; the length of the fiber in agglomeration area was 42 mm; the elastic modulus E of the fiber was 2,224.6 cN/tex; the shear elastic modulus G of the fiber was 106.2 cN/tex; the density of the fiber was 1,510 kg/m^3; the number of fiber division units was 500; the left lateral angle was 15°; the initial position of the fiber in lateral entry compact

spinning with suction groove was Z=-1 mm; the initial position of the fiber in intermediate entry compact spinning with suction groove and ring spinning was Z=0 mm; The time integral step was 10–6s.

Then, the initial parameters will type in the MATLAB finite fiber simulation model.

3.2. Simulation results and analysis

According to the specific value, we calculated the fiber motion in the agglomeration area by MATLAB software.

Figure 6 shows the movement of single fiber. It is obvious that lateral entry compact spinning with pneumatic groove spinning twisted obviously than intermediate entry compact spinning with suction groove spinning or the ring spinning. And, ring spinning almost has no additional twist. Because of the lateral direction of fiber bundle during the agglomeration area, the fiber, especially the edge fiber, would move closer to the center. The fiber bundle would be more inseparable, and it would improve the yarn properties.

The condensing zone is for better gathering fiber. And, the best condition is that when the fiber bundle is totally gathered in this place and the twist form is to be cylinder. Then, the yarns

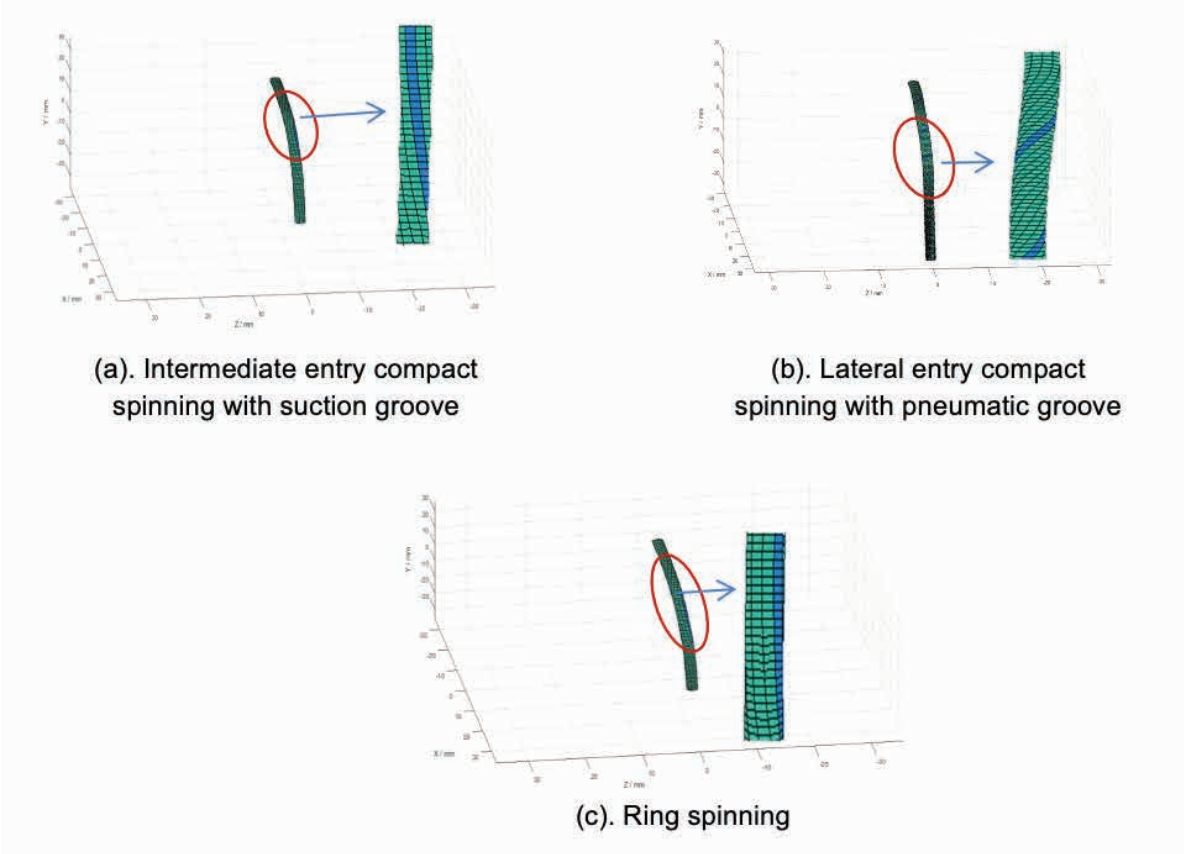

Figure 6. Single fiber movement of three kinds of spinning

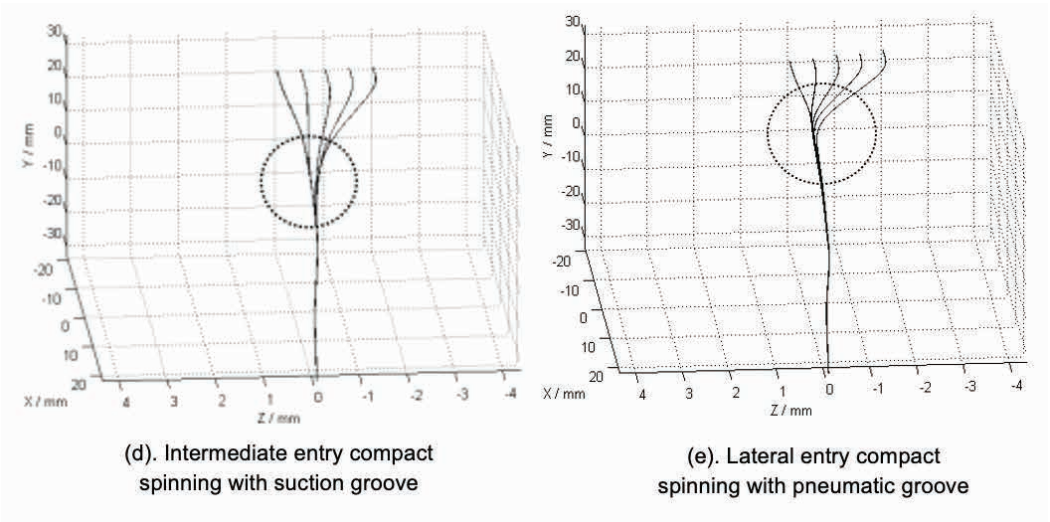

Figure 7. Fiber motion of two kinds of compact spinning

will avoid the triangle, and the yarn properties will be better. Figure 7 shows the fiber motion of two compact spinning. As Figure 3 shows, the x,y coordinate of the condensing zone is from A(20,10)mm to B(10,-20)mm. Figure 7 (d) shows the fiber motion of intermediate entry compact spinning with suction groove and (e) shows the fiber motion of lateral entry compact spinning with pneumatic groove. In Figure 7 (d), the fiber is totally condensing during the x,y coordinate of (10,-20) mm and (e) is (15,-10) mm. The fiber of lateral entry compact spinning with pneumatic groove is totally condensed during the condensing zone but the fiber of intermediate entry compact spinning with suction groove is condensing at the edge of condensing zone. Fiber bundles will not get total gathered in case (d). The twists of spindle will pass forward and breakdown the gathered fiber bundles. Finally, the twist triangle cannot be avoided. It will lead the yarn hairiness and the final yarn properties worse. At in the case of Figure 7 (e), the fiber bundle will totally be gathered during the condensing zone. The output fiber bundle looks like near-cylindrical, and the yarn will be tighter, and the hairiness will less after twisted.

4. Results and discussion

In order to compare the yarn properties of the lateral entry compact spinning with pneumatic groove, intermedia entry compact spinning with suction groove and ring spinning, the yarns were spun, and the yarn properties tests were carried out. The spinning machine and raw materials used in the experiment were, respectively, provided by two different companies (Hunan Huashen Group and Ningbo Dechang Precision Textile Machinery CO., LTD). The spinning yarn was 36 Nm ramie yarn. According to the experimental program, the twist, strength, and hairiness of yarn were compared. During the experiment, the experimental test instruments were unchanged.

4.1. Basic experimental parameters and testing instruments

The raw material was ramie roving. The mass of the roving was 4.70 g/10m; the moisture regain of the roving was 8.07%. All the spinning was finished by the domestic FZ501-type spinning machine. The pressure of pneumatic groove was -2,600 (Pa), the twist was 680 (T/m), the spinning speed was 7,000 (r/min). The count of yarn was 36 Nm.

The tests were performed at the standard atmosphere pressure, when the relative humidity was 65%±3% and the temperature was (20±2)℃. Before testing, the specimen should be humidified for 48 hours in a constant temperature and humidity laboratory. The type of yarn evenness test instrument was UT4 evenness meter. Uster UT4 adopts capacitive sensor and photoelectric sensor to measure yarn diameter unevenness, slub, detail, and ramie yarn number. The test speed is 400 m/min, and each tube yarn was tested 10 replications. The yarn tension of different counts was adjusted by (0.5±0.1) cN/tex. The tested specimens were 3 kinds of bobbins that have 10 replications per bobbin when tested. The type of the yarn hairiness test instrument was YG172A yarn hairiness tester. The testing condition is according to FZ/T01086-2000 [12]. During the yarn hairiness tests, the length of the test fragment was 10 m, the number of tests was 1 tube per 10 times. The test speed was 10 m/min. The type of yarn strength test instrument was YG063T, according to GB/T4711-1984 [13]. During the yarn strength test, the clamp distance was 500 mm, and the tested speed was 500 mm/min. The type of yarn twist test instrument was YG331A yarn twist test tester. According to GB/T2543.2-2001 [14], the experiment adopted a method of untwist-retwist method, which was to test the yarn with a certain length under the specified tension and measure the number of rounds when returning to the starting length after untwisting and reversed twisting. The experiment used counterclockwise running direction, the speed was 800 r/min, the length of the sample was 500 mm, and the pre-tension was calculated according to the formula of the yarn $1.8\sqrt{\mathrm{Tt}} - 1.4\mathrm{cN}$. The allowable elongation limit was 4.0 mm. For the mean±sd (standard deviation), the standard deviation was mainly decided by the test equipment and environment.

4.2. Comparison of yarn evenness

The essence of yarn linear density unevenness is the unevenness of fiber arrangement along the length direction in the yarn sliver. It is an important factor that directly affects the yarn breaking strength and elongation, yarn twist distribution, and yarn thickness unevenness. Therefore, it is very important to measure the evenness of yarn.

In Table 1, all the indicators of II are best. On calculation, CVm of II has reduced 7.32% compared to that of I and reduced 20.4% compared that of III. The thick place and the thin place have the same tendency. The lateral entry compact spinning with pneumatic groove could improve the parallelism of fiber arrangement. In the meantime, the reduction of thick place and thin place will lead the yarn more evenness.

Table 1. Yarn evenness.

Yarn types	CVm/%	Thick place (+50%) (/km)	Thin place (-50%) (/km)	Nep number (/km)
I	19.80	198	130	276
II	18.35	183	112	195
III	23.06	210	155	380

Note: I as intermediate entry compact spinning with suction groove, II as lateral entry compact spinning with pneumatic groove, and III as ring spinning.

4.3. Comparison of yarn strength

Yarn strength is an important technical indicator of yarn quality assessment. It has a positive meaning to guide the production, formulation, and adjustment of the spinning process through testing of yarn strength.

In Table 2, the yarn breaking strength was increasing for the lateral compact spinning with pneumatic grooves. For the same count yarn, the strength of the lateral compact spinning with pneumatic grooves spinning yarn was the highest. Because it is gathered in the condensing zone and is totally assembled in this place, the output fiber bundle is tighter and so the final yarn. With highly gathered, the yarn could resist the external force and had the highest breaking tenacity. And, the breaking elongation of these types of spinning was almost the same. It showed that compact spinning could not improve the ramie yarn's breaking elongation.

4.4. Comparison of yarn hairiness

Yarn hairiness is one measure of the yarn quality. The reduction in hairiness is a key indicator of this test and is the biggest advantage of compact spinning. While not all hairiness is harmful, in a certain range, the shorter hairiness can smooth the appearance of the yarn and fabric. In this paper, the hairiness length above 3 mm is regarded as the main basis of evaluate the effect of spinning experiment.

The tested number of hairiness length was 1–10 mm and 4–10mm was compared. From Table 3, the number of hairiness of length 4–10mm for I, II was significantly less than III. Comparing the yarn hairiness of I, II, it also showed that the hairiness of II was better than I. The hairiness of I was 72.39% lower than III, and the hairiness of II was 80.21% lower than III. Compared with I, II, the hairiness of II was 28.46% lower than I. So, the reduction of hairiness of lateral entry compact spinning with pneumatic groove was the best. The ramie yarn had high hairiness because of its high stiffness and low elongation. The lateral entry compact spinning with pneumatic groove made the free-end fibers on the edge attached to the yarn more efficient. Therefore, the hairiness was lower. Through the compact spinning, the hairiness of ramie yarn reduced. It was good for the finishing process and the post-procedure process.

To comment on the degree of difference between the average values of yarn hairiness of I and II, the statistic t is calculated as follows:

$$t = \frac{|\bar{X}_1 - \bar{X}_2|}{\sqrt{\frac{\sum x_1^2 + \sum x_2^2}{n_1+n_2-2} \times \frac{n_1+n_2}{n_1 \times n_2}}} \quad (11)$$

where $\bar{X}_1$ is the average value of I, $\bar{X}_2$ is the average value of II, n1 is the number of I, n2 is the number of II, and n1=n2=30. The degree of freedom is df=n–1=29, and t=0.000<t (29)0.05 from the t critical values. According to this, the spinning method of lateral entry compact spinning with pneumatic groove and intermediate entry compact spinning with suction groove has a statistically significant effect on the yarn hairiness.

Table 2. Yarn strength.

Yarn types	Breaking tenacity/cN/tex	Breaking tenacity CV/%	Breaking Elongation /%	Elongation CV/%
I	27.7	11.19	3.1	7.09
II	29.4	9.99	3.1	6.95
III	26.4	14.81	3.2	9.46

Table 3. Yarn hairiness.

Yarn types	1 mm	2 mm	3 mm	4 mm	5 mm	6 mm	8 mm	10 mm	Total of 4–10mm	Reduced hairiness compared to ring spinning
I	531.7	205.7	99.3	47.7	25.3	13.3	6.3	3.3	95.9	72.39%
II	465.3	186.3	86.6	40.4	15.3	8.3	3.7	1.3	68.6	80.21%
III	910.8	473.8	278.3	150.8	84.3	56.0	35.8	19.8	346.7	/

Table 4. Yarn twist.

Twist (T/m)	1	2	3	4	5	6	7	8	9	10	Average
I	548	555	557	587	550	570	585	586	566	573	567.7
II	630	645	635	643	641	633	639	637	643	645	639.1
III	539	524	524	530	552	550	578	567	550	527	547.7

Note: I as intermediate entry compact spinning with suction groove, II as lateral entry compact spinning with suction groove, and III as ring spinning.

4.5. Comparison of yarn twist

Yarn twist is a major factor that will affect the yarn strength. However, the unreasonable twist will lead to some problems. Yarn twist will lead to the hairiness problems and the later process, such as weaving.

As seen in Table 4, all the twists were below the designed twist, but the twist of lateral compact spinning with suction grooves was highest. The loss of twist was attributed to the low elongation and high stiffness of ramie. During the spinning time, because of the high stiffness and low elongation, the fiber was harder to be twisted and easily broken than cotton fibers. The lateral entry compact spinning with pneumatic groove could reduce the loss of twist.

The next 3 figures showed the yarn forms of the three different spinning methods.

Figure 8. Yarn of intermediate entry compact spinning with suction groove spinning

Figure 9. Yarn of lateral entry compact spinning with suction groove spinning

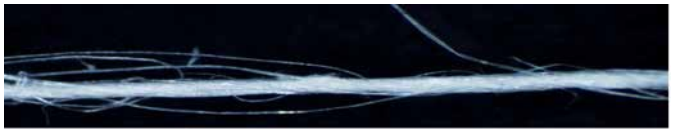

Figure 10. Yarn of ring spinning

5. Conclusions

Compact spinning is the consequence of airflow and mechanical actions on fibers. The new finite element method simulates the fiber motion during the fiber bundle through the agglomeration area and proves that the lateral groove can gathered the fiber bundle efficiently during yarn agglomeration. From the simulation results, the gathering point of the lateral compact spinning with pneumatic groove is assembling in the gathering area, and it can be a better cluster fiber. The experiment results fit the numerical analysis: The yarn of lateral compact spinning with pneumatic groove has better shape and properties. When the fiber is getting through condensing zone of the lateral groove, the fiber bundle can be arranged into the ideal shape, and after twisting the yarn, it can get better yarn properties. Compared with the intermediate compact spinning with suction groove, the lateral compact spinning with pneumatic groove can reduce yarn hairiness and increase yarn strength, thus improving the overall performance of the yarn.

Acknowledgments

This work was supported by the National Key R&D Program of China under Grant [number 2017YFB0309100] and the China Scholarship Council.

References

[1] Lawrence CA. (2003). Twist and twist factor. Fundamentals of Spun Yarn Technology. CRC Press (Florida).

[2] Li, E. M., Hua, Z. H., Xue, W. L. (2016). Finite-element method of statics analysis of the geometric large deformation of fiber elastic thin rod models. Donghua Uniy (Nat Sci), 6, 916-921.

[3] Kong, L. X., Platfoot, RA. (1997). Computational two-phase air flow within transfer channels of rotor spinning machines. Textile Research Journal, 67(4), 269-278.

[4] Guo, H.F. (2009). Research on three-dimensional rotating airflow field and flexible fiber motion in air-jet spinning nozzle. PhD Thesis, Donghua University, China.

[5] Bangert, L. H., Sagdeo, P. M. (1977). On Fiber Alignment Using Fluid-Dynamic Forces Textile Research Journal, 47, 773-780.

[6] Cheng, D. W. (1985). Discrimination of the possibility of various motion modes of fibers in fluid. Donghua Uniy (Nat Sci), 2, 1-8.

[7] Cheng, D. W. (1987). Discrimination of the plane motion of curved fiber. Donghua Uniy (Nat Sci), 06, 73-78.

[8] Yamamoto, S., Matsuoka, T. (1993). A method for dynamic simulation of rigid and flexible fibers in a flow field. Journal of Chemical Physics, 98(1), 644-650.

[9] Liu, Y. Z. (2006). Nonlinear mechanics of elastic thin rods. Tsinghua University Press (Beijing).

[10] Zhang, Y., Zeng Y. C., Wang Y. X. (2013). Fiber motion in nozzle flow field of vortex spinning based on bead rod model. Donghua Uniy (Nat Sci), 39(05):583-589.

[11] Wang Y., Zou Z. Y., Hua Z. H. (2009). Simulation and analysis of trajectory of fiber in condensing zone of compact spinning with lattice apron. 30(10):48-52.

[12] FZ/T 01086-2000. Textiles -Test method for yarn hairiness.

[13] GB/T 4711-1984. Wool yarns.

[14] GB/T 2543.2-2001. Textiles -Determination of twist in yarn-Part2: Untwist-retwist method.